Ullah, I., Wagih, M. and Beeby, S. (2022) A Wearable Backscattering Modulator and RF Energy Harvester for UHF RFID Applications. In: 29th IEEE International Conference on Electronics, Circuits and Systems (ICECS 2022), Glasgow, UK, 24-26 Oct 2022, ISBN 9781665488235.

A Wearable Backscattering Modulator and RF Energy Harvester for UHF RFID Applications

1st Irfan Ullah
School of Electronics and Computer Science
University of Southampton
Southampton, UK
i.ullah@soton.ac.uk

2nd Mahmoud Wagih
James Watt School of Engineering
University of Glasgow
Glasgow, UK
mahmoud.wagih@glasgow.ac.uk

3rd Steve Beeby
School of Electronics and Computer Science
University of Southampton
Southampton, UK
spb@ecs.soton.ac.uk

***Abstract*—To enable remote, battery-free, and wearable healthcare, ultra-low-power and highly-efficient energy harvesting and communication front-ends are required. This paper presents the design and implementation of a wearable backscattering modulator and RF energy harvester for UHF RFID applications, which represents the first textile-based RFID modulator. The measured performance of the modulator is characterized using s-parameters and is shown successfully communicating with a commercial RFID reader using a textile antenna, suitable for integration in a fabric bandage. The rectifier's efficiency is also presented, in presence of the modulator, showing a high RF to DC efficiency exceeding 50%. This work lays the foundation for UHF RFID-powered smart bandages for next generation healthcare applications.**

***Index Terms*—UHF RIFD sensor, wearable backscattering modulator, RF energy harvester, RF energy, wearable sensors, WISP 5**

I. INTRODUCTION

The demand for wearable sensors for healthcare applications has significantly increased in recent years. These sensors continually monitor users' health and provide useful information to health practitioners to improve personalized healthcare [1], [2]. For example, smart bandages are integrated with electronics to provide real-time information about chronic non-healing wounds, such as temperature, moisture, and pH level. The energy source to power wearable sensors is crucial. Most wearable devices are usually powered by batteries. Batteries are generally bulky and rigid and have a finite lifetime and therefore, less suitable for designing wearable sensors. Ultra-High Frequency (UHF) Radio Frequency Identification (RFID) is one of the most promising technologies to solve such problems.

A typical UHF RIFD system mainly consists of an interrogator (reader) and a transponder (tag). Rectifier and modulator circuits are the key components in designing RFID tag chips. The rectifier is used to harvest RF power while a modulator performs the backscatter modulation to the reader. A standard tag chip comes in a die form and is used for various applications such as logistics, goods and asset tracking, monitoring and indoor localization. However, these microchips cannot execute arbitrary computer programs and do not support sensors, making them less suitable for exploring new sensor integration applications.

There are fully customisable and programmable UHF RFID sensing platforms that include a programmable microcontroller and arbitrary sensors, enabling novel RFID applications [3]. For example, the Wireless Identification and Sensing Platform (WISP) [4], [5] is a programmable passive platform for low-power sensing applications. Arbitrary sensors can be integrated into this platform and can be optimised for different sensing applications. The platform is battery-free and therefore, harvests energy from electromagnetic waves transmitted by the reader antenna. So far, the WISP platform has been optimised for various applications such as temperature [4], designing backscatter-based cameras [6], battery-free HD video streaming [7] for neural interface [8] and capacitive touch interface [9], and for designing photovoltaic enhanced UHF RFID tag antennas [10]. Nevertheless, there has been no report to date of a UHF RFID modulator implemented on flexible wearable materials [11], e.g. smart textiles or fabric bandages.

In this paper, we propose a wearable modulator and RF energy harvester for UHF RFID applications. The modulator can be used in customizable and programmable UHF RFID-based sensors for wearables applications. The modulator is fabricated using flexible polyimide laminate and polyester felt textile. The power conversion efficiency (PCE) of the rectifier and modulator is investigated, showing an efficiency of 50% at the optimal load resistance of $3\,\mathrm{k\Omega}$ for different input power levels, with and without the modulator. A successful read is demonstrated with a commercial Gen-2 UHF RFID reader showing that computational RFID platforms could be used in wearable healthcare applications.

II. CIRCUIT DESIGN

A. Rectifier Design

The schematic and layout mask of the rectifier with a modulator is illustrated in Fig. 1(a) and (b), respectively, and the values of the components are given in Table 1. The matching network consists of two inductors, L_1 of $22\,\mu\mathrm{H}$ and L_2 of $47\,\mu\mathrm{H}$, which were optimised to match the input impedance to 50 ohms to maximise the power conversion efficiency. The rectifier circuit design is based on the voltage doubler topology which provides a much higher voltage conversion ratio. The output voltage doubler is composed of the *SMS7630* [12] rectifying diodes D_1 and D_2 and two charge capacitors C_1 and

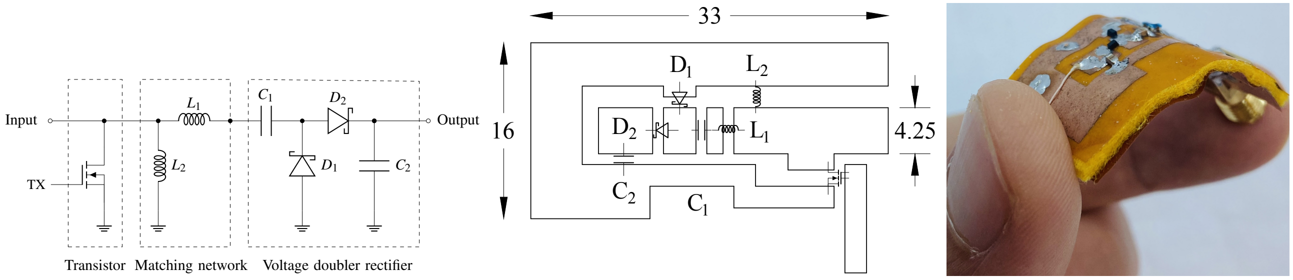

(a) (b) (c)

Fig. 1: (a) Schematic and (b) final layout mask illustration of the proposed flexible textile-based rectifier with a modulator design for UHF RFID applications and (c) prototype of the textile-based rectifier with the modulator design.

TABLE I: LUMPED COMPONENT VALUES USED IN DESIGNING THE MODULATOR CIRCUIT.

Component	Value
MOSFET	3SK293
L_1	22 µH
L_2	47 µH
C_1, C_2	100 pF
D_1, D_2	SMS7630

C_2. A Schottky diode was chosen due to its high-frequency operation and lower threshold voltage. The function of the charge capacitors is to boost the peak and smooth the output dc voltage. The circuit was designed using PathWave Advanced Design System (ADS) by Keysight Technologies [13].

B. Modulator Design

The modulator design consists of a microstrip line with an impedance of 50 ohms and a MOSFET. The dual gate N-channel MOSFET, *3SK293* [14], from Toshiba is used in which the drain terminal is connected to the microstrip line, the source terminal is connected to the ground and the gates are connected to the *TX* pin of the microcontroller. The backscattering modulation technique is based on the variation of the reflection coefficient (S_{11}) at the input of the tag antenna.

III. MEASUREMENTS AND RESULTS

A. RF-DC Energy Harvesting Efficiency

The design, Fig. 1(b), was etched on a 25 µm thick polyimide laminate sheet [15], and 1 mm thick polyester felt was sandwiched between the design layout and the ground plane, as shown in Fig. 1(c). Two designs were prepared: (i) a rectifier design and (ii) a rectifier design with the modulator. The performance of the rectifier and modulator were evaluated with a two ports vector network analyzer, Rhode and Schwarz ZVB4 [16]. Fig. 2(a) shows the reflection coefficient, S_{11}, of both circuits for input RF power levels of 0 and 10 dBm. It can be observed that the rectifier circuit resonates at 1 GHz, and the S_{11} is −25 dB for the input power of 10 dBm, while the resonance frequency of the rectifier in the presence of the modulator is slightly shifted to a high frequency of 1.3 GHz. However, both circuits are resonant at 1 GHz when the input power is 0 dBm.

Additionally, the efficiency of the circuits was also investigated for different load impedance ranging from 0.1 to 100 kΩ and frequency of 915 MHz. The efficiency of the circuits was calculated with the following equation [17]:

$$\eta_{RF-DC} = \frac{P_{DC}}{P_{RF}} \times 100\% = \frac{V_{DC}^2/R}{P_{RF}} \times 100\% \tag{1}$$

where P_{DC} is output dc power which is equal to the square of the output dc voltage (V_{DC}) divided by resistive load present at the output (R) and P_{RF} is input RF power.

Fig. 2(b) depicts the measured efficiency performance of both circuits, indicating that the rectifier exhibits an efficiency above 50% for an optimum load of 3 kΩ. However, the optimum load efficiency of the modulator is slightly lower than the rectifier. For 10 dBm input power, the efficiency of the modulator significantly declined which is 38%. This is due to a shift in the resonance frequency to 1.3 GHz of the modulator when the input power is 10 dBm. Additionally, the output dc voltage against the input power levels of the circuit was also measured for no-load impedance and the optimum load impedance of 3 kΩ, and the measured results are summarised in Fig. 2(b).

Furthermore, the dc voltage against the input RF power levels from −10 to 10 dBm for no load and optimum load at 915 MHz is given in Fig. 2(c). It is evident that the output dc is increasing as the input power increases, as expected. It can be noted that the output dc voltage of the rectifier is slightly higher than the modulator circuit. For no-load impedance, the output dc voltage is higher than the optimum load impedance.

B. Modulator Testing

The setup, Fig. 3(a), was prepared to test the proposed modulator design. The setup consists of textile-based proximity coupled patch antenna, a modulator, a demodulator, an MSP430FR5969 microcontroller and an accelerometer as a sensor. The textile-based patch antenna resonates in the

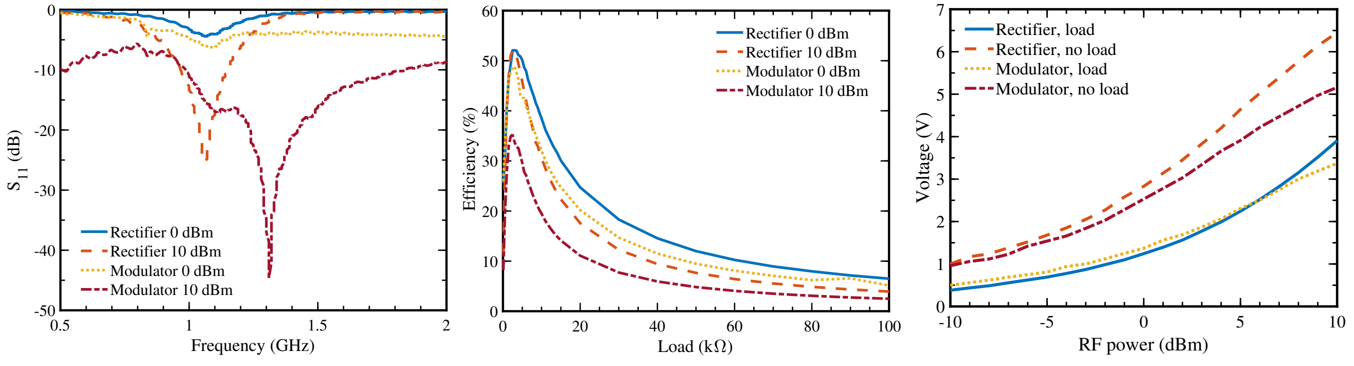

(a) (b) (c)

Fig. 2: (a) Measured reflection coefficient, S_{11} and (b) efficiency versus different load impedance of the rectifier and modulator at different input power levels at $915\,\mathrm{MHz}$ frequency. (c) Output dc voltage of the rectifier and the modulator against different input power levels from -10 to 10 dBm for no-load impedance and optimum load impedance of $3\,\mathrm{k\Omega}$ at $915\,\mathrm{MHz}$ frequency.

$915\,\mathrm{MHz}$ UHF band and is coupled with the modulator using a straight RF adapter SMA plug. The microstrip patch antenna with proximity coupled $50\,\Omega$ feeding line is implemented in two layers of $1\,\mathrm{mm}$ thick polyester substrates and the dimensions of the patch are altered to operate at $915\,\mathrm{MHz}$. The gates of the transistor were connected to the *TX* pin of the microcontroller while the *RX* pin of the microcontroller is connected to the demodulator. The sensor communicates with the microcontroller using the SPI protocol. The setup is based on the latest version of the WISP 5.1 which hardware and firmware are available in [18]. The setup appears as a tag chip to the RFID reader. The Impinj R420 UHF RFID reader [19] with an 8.3 dBi gain antenna was used to interrogate the sensor. Fig. 3(b) shows the transmitted Electronic Product Code (EPC) of the sensor in response to the RFID query, showing the successful backscatter communication of the proposed modulator to the RFID reader.

IV. CONCLUSION

In this paper, a flexible textile-based modulator design for the UHF RFID application has been demonstrated. The modulator design can be used for RF energy harvesting for designing wireless and battery-free sensors for wearable applications. Measurements were performed to investigate the optimal efficiency and load resistance for both circuits, rectifier and modulator. The results show that the rectifier exhibits an efficiency of 50% for input power levels of 0 and 10 dBm at $915\,\mathrm{MHz}$ while the calculated efficiency of the modulator is 48%. The rectifier circuit resonates at around $1\,\mathrm{GHz}$ but still, good efficiency of 50% is achieved at $915\,\mathrm{MHz}$, indicating that the rectifier can be used as an RF energy harvester for UHF RFID applications. The modulator was experimentally validated with the sensor setup and the sensor setup has successfully transmitted EPC to the RFID reader at the $915\,\mathrm{MHz}$ UHF band. The significance of the proposed design is that it is made of $25\,\mu\mathrm{m}$ flexible polyimide laminate and polyester felt and therefore, can be easily integrated into textiles for wearable applications.

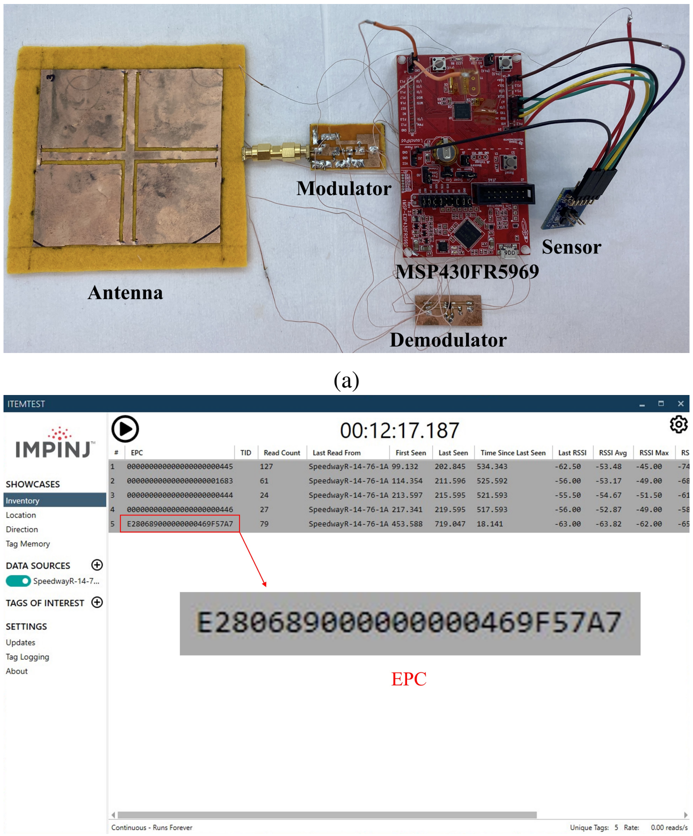

00:12:17.187

#	EPC	TID	Read Count	Last Read From	First Seen	Last Seen	Time Since Last Seen	Last RSSI	RSSI Avg	RSSI Max	RS
1	000000000000000000000445		127	SpeedwayR-14-76-1A	99.132	202.845	534.343	-62.50	-53.48	-45.00	-74
2	000000000000000000001683		61	SpeedwayR-14-76-1A	114.354	211.596	525.592	-56.00	-53.17	-49.00	-68
3	000000000000000000000444		24	SpeedwayR-14-76-1A	213.597	215.595	521.593	-55.50	-54.67	-51.50	-61
4	000000000000000000000446		27	SpeedwayR-14-76-1A	217.341	219.595	517.593	-56.00	-52.87	-49.00	-58
5	E2806890000000000469F57A7		79	SpeedwayR-14-76-1A	453.588	719.047	18.141	-63.00	-63.82	-62.00	-65

E2806890000000000469F57A7

Continuous - Runs Forever

Unique Tags: 5 Rate: 0.00 reads/s

(a)

(b)

Fig. 3: (a) Setup for testing the proposed modulator design and (b) successful interrogation showed via the transmitted Electronic Product Code (EPC) from the wearable modulator to the RFID reader at $915\,\mathrm{MHz}$.

ACKNOWLEDGMENT

This work was supported by European Regional Development Fund (ERDF) via its Interreg V France (Channel) England programme: Smart Textile for Regional Industry and

Smart Specialisation Sectors (SmartT). M. Wagih was supported by the Royal Academy of Engineering and the Office of the Chief Science Adviser for National Security under the UK Intelligence Community Postdoctoral Research Fellowship programme. The work of Steve Beeby was supported by the Royal Academy of Engineering under the Chairs in Emerging Technologies Scheme.

REFERENCES

[1] M. M. Rodgers, V. M. Pai and R. S. Conroy, "Recent advances in wearable sensors for health monitoring," *IEEE Sensors J.*, vol. 15, no. 6, pp. 3119–3126, June 2015.

[2] T. Wu, F. Wu, C. Qiu, J. -M. Redouté and M. R. Yuce, "A rigid-flex wearable health monitoring sensor patch for IoT-connected healthcare applications," *IEEE Internet of Things J.,* vol. 7, no. 8, pp. 6932–6945, Aug. 2020.

[3] F. Muralter, L. Arjona, H. Landaluce and A. Perallos, "A fully customizable RFID research platform with exchangeable Mmdules" in *IEEE Sensors J.,* vol. 21, no. 13, pp. 15379–15385, July, 2021.

[4] A. P. Sample, D. J. Yeager, P. S. Powledge, A. V. Mamishev and J. R. Smith, "Design of an RFID-based battery-free programmable sensing platform," *IEEE Trans. Instrum. Meas.,* vol. 57, no. 11, pp. 2608–2615, Nov. 2008.

[5] Smith, J.R., Sample, A.P., Powledge, P.S., Roy, S., Mamishev, A. (2006). " A Wirelessly-powered platform for sensing and computation," In: Dourish, P., Friday, A. (eds) UbiComp 2006: Ubiquitous Computing. UbiComp 2006. Lecture Notes in Computer Science, vol 4206. Springer, Berlin, Heidelberg.

[6] S. Naderiparizi, Z. Kapetanovic and J. R. Smith, "RF-powered, backscatter-based cameras," *11th European Conf. on Antennas and Propag. (EUCAP),* 2017, pp. 346–349.

[7] Naderiparizi, Saman, Mehrdad Hessar, Vamsi Talla, Shyamnath Gollakota, and Joshua R. Smith. "Towards battery-free HD video streaming," *15th USENIX Symposium on Networked Systems Design and Implementation (NSDI 18),* pp. 233–247. 2018

[8] D. J. Yeager, J. Holleman, R. Prasad, J. R. Smith and B. P. Otis, "NeuralWISP: a wirelessly powered neural interface with 1-m range," *IEEE Trans. Biomed. Circuits Syst.,* vol. 3, no. 6, pp. 379–387, Dec. 2009.

[9] A. P. Sample, D. J. Yeager and J. R. Smith, "A capacitive touch interface for passive RFID tags," *IEEE Int. Conf. on RFID,* 2009, pp. 103–109.

[10] A. P. Sample, J. Braun, A. Parks and J. R. Smith, "Photovoltaic enhanced UHF RFID tag antennas for dual purpose energy harvesting," *IEEE Int. Conf. on RFID,* 2011, pp. 146–153.

[11] A. Komolafe, et al. "Integrating flexible filament circuits for e-textile applications," *Adv. Mater. Technol.* 4.7 (2019): 1900176.

[12] Skyworks (July 15, 2022), SMS7630 series, surface mount mixer and detector schottky diodes. [Online]. Available: https://www.skyworksinc.com/Products/Diodes/SMS7630-Series.

[13] Keysight (July 16, 2022), PathWave Advanced Design System (ADS). [Online]. Available: https://www.keysight.com/us/en/products/software/pathwave-design-software/pathwave-advanced-design-system.html

[14] Toshiba, (July 15, 2022), 3SK293 high frequency MOSFET. [Online]. Available: https://toshiba.semicon-storage.com/eu/semiconductor/product/mosfets/detail.3SK293.html.

[15] GTS flexible by design, (July 15, 2022), GTS7800-copper polyimide laminates. [Online]. Available: https://www.gtsflexible.com/.

[16] Rohde & Schwarz (July 15, 2022), R&S ZVB4 vector network analyzer 4 ports, 4 GHz. [Online]. Available: https://www.rohde-schwarz.com/nl/product/zvb4-4-port-productstartpage_63493-9747.html.

[17] B. Gyawali, S. K. Thapa, A. Barakat, et al. "Analysis and design of diode physical limit bandwidth efficient rectification circuit for maximum flat efficiency, wide impedance, and efficiency bandwidths," *Sci. Rep.* 11, 19941 (2021).

[18] WISP 5 firmware repository. [Online]. Available: https://github.com/wisp/wisp5

[19] Impinj (July 15, 2022), Impinj speedway rain RFID readers for flexible solution development. [Online]. Available: https://www.impinj.com/products/readers/impinj-speedway.